Molecular Crystals and Liquid Crystals

ISSN: 1542-1406 (Print) 1563-5287 (Online) Journal homepage: http://www.tandfonline.com/loi/gmcl20

Effect of NaCl Concentration on Silver Nanoparticles Produced by 1064 nm Laser Ablation in NaCl Solution

Mozhdeh Sharif & Davoud Dorranian

To cite this article: Mozhdeh Sharif & Davoud Dorranian (2015) Effect of NaCl Concentration on Silver Nanoparticles Produced by 1064 nm Laser Ablation in NaCl Solution, Molecular Crystals and Liquid Crystals, 606:1, 36-46, DOI: 10.1080/15421406.2014.915620

To link to this article: http://dx.doi.org/10.1080/15421406.2014.915620

Published online: 15 Jan 2015.

Mol. Cryst. Liq. Cryst., Vol. 606: pp. 36–46, 2015

ISSN: 1542-1406 print/1563-5287 online
DOI: 10.1080/15421406.2014.915620

Effect of NaCl Concentration on Silver Nanoparticles Produced by 1064 nm Laser Ablation in NaCl Solution

MOZHDEH SHARIF[1] AND DAVOUD DORRANIAN[2,*]

[1]Department of Physics, Science Faculty, Islamic Azad University Central Tehran Branch, Tehran, Iran
[2]Laser Lab., Plasma Physics Research Center, Science and Research Branch, Islamic Azad University, Tehran, Iran

Silver nanoparticles (NPs) were synthesized by laser (Nd:YAG, 1064 nm) ablation of a silver target in various concentrations of NaCl solutions as well as in distilled water. The optical properties, size distribution, and agglomeration of NPs were investigated by several diagnostics. The UV–Vis-NIR absorption spectrum of the Ag NPs exhibits absorptions in the ultraviolet and visible regions because of interband transition and surface plasmon resonance oscillations of Ag NPs, respectively. The average size of produced particles is increased as concentrations of NaCl in the solutions increases. TEM and SEM micrographs were used to study the size distribution and morphology of NPs. TEM images indicate that the aggregation of NPs in NaCl solutions is more than distilled water.

Keywords Absorption; neodymium YAG laser; pulsed laser ablation (PLA); SEM; silver nanoparticles; surface plasmonic resonance; TEM; XRD

1. Introduction

Recently, pulsed laser ablation (PLA) of bulk target immersed in liquid environment which is a simple method to prepare metal nanoparticles (NPs) has attracted much attention since they exhibit different optical, magnetic, and electric properties from bulk materials [1, 2]. The PLA method has attracted attention due to its enormous potential in laser-based materials processing, such as nanocrystals growth, solid thin film, surface cleaning, and microelectronic devices fabrication. In addition, the PLA technique offers advantages in preparation methodology: (I) "simple and clean" synthesis, (II) ambient conditions without extreme temperature and any special physical conditions such as pressure, and (III) formation of NPs that may occur in both liquid and solid forms [3]. Nanoscale materials, as an intermediate state between molecular and bulk materials, possess unique chemical and physical properties that drive significant fundamental and technological interest [4]. Materials characteristics drastically change as the size of the constituting particles approaches the nanoscale regime [4]. The change in properties is a result of the presence of a small number

*Address correspondence to Davoud Dorranian, Laser Lab., Plasma Physics Research Center, Science and Research Branch, Islamic Azad University, Tehran, Iran. E-mail: doran@srbiau.ac.ir

Color versions of one or more of the figures in the article can be found online at www.tandfonline.com/gmcl.

of atoms in each particle and a large surface-to-volume ratio due to the large fraction of atoms that reside on the particle surface [4].

The size-dependent properties of silver NPs make them suitable for many applications in various areas such as catalytic, optical, and antibacterial applications [5, 6]. The optical absorption spectra of metal NPs are evident as shown by surface plasmon resonance (SPR) [7]. For metal NPs the SPR, which occurs in the visible wavelengths, is sensitive to size, shape, and the surrounding media [8]. Ag NPs are well known to have a SPR at approximately 400 nm, with the wavelength dependent on the size and shape of Ag NPs [9]. It has been demonstrated that laser irradiation onto gold or silver NPs dispersed in aqueous solution-induced fragmentation or fusion of the colloidal NPs [10–14]. The photo thermal dynamics involved in these processes has been also extensively investigated [15–18]. However, the shape of the produced NPs was almost spherical whatever the shape of the original NPs.

In this work, we will present our data on the fabrication of silver NPs by laser ablation method in NaCl solution and effect of the concentration of NaCl in the solution on the properties of Ag NPs is investigated. The manuscript is organized as follow; following the introduction in section 1, experimental setup is introduced in section 2. Section 3 is devoted to results and discussion and section 4 includes conclusion.

2. Experimental Setup

Silver NPs were produced by laser ablation of a bulk silver plate in distilled water and NaCl solution with different concentrations. As is shown in Fig. 1, the silver bulk plate of 3 mm thickness (>99.5%) was cleaned with ethanol and deionized water.

The cleaned target was placed at the bottom of a glass vessel containing 20 mL distilled water. The target was kept at 12 mm depth in the liquid. The metal plate was ablated with the output of the fundamental pulse (1064 nm) of Quanta-ray Nd:YAG laser operating at 2 Hz repetition rate and 7 ns pulse width. The laser beam was focused on the surface of

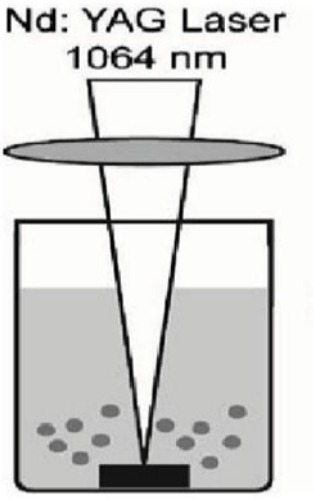

Figure 1. Schematic diagram of experimental setup.

target with a 80 mm focal length lens. The spot size of laser beam on the surface of silver target was calculated to be 30 μm. The laser fluence was 5 J/cm^2 with 6 mm in diameter spot size (before lens). Upon irradiation of the laser beam, the solution gradually turned to dark yellow. Four concentrations of 0, 5, 10, and 15 mM of NaCl solution was selected as the ablation environment. The variety of analytical techniques was employed to characterization of products. The absorption spectrum of nanoparticle suspensions were examined at room temperature by a UV–Vis-NIR absorption spectrophotometer PG instruments (T-80). Transmission electron microscopy (TEM, zeiss-Em10C-80 KV) was obtained by placing a drop of the concentrated suspension on a carbon-coated copper grid to show us the morphology and size of NPs. Scanning electron microscopy (SEM) micrographs were prepared with (SEM, KYKY-EM3200, English Malvern Co.) device from PHILIPS Co. (Philips from China) X-ray diffraction was measured employing Philips-PW3710. DLS measurement was done using the ZETASIZER-HSA300 device from English MALVERN Co. for studying the size distribution of the NPs in solutions. Normally, lots of particles were counted to determine the size distribution of each sample. Room temperature photoluminescence (PL) of the samples with (PL, Luminescence Spectrometer—Ls-5) device from USA PERKIN ELMER Co. was measured to characterize the luminescence properties of the NPs. To investigate the molecular bonds in the suspensions, the Fourier transform infrared spectroscopy FT-IR (FTIR, NEXUC870) system was used. To measure the ablation rate in the liquid medium, the target was weighed up before and after the ablation process by an accurate scale Satorius model CP225D with 0.01 mg readability.

3. Results and Discussion

Picture of nanoparticle solution are presented in Fig. 2. As we know, the light yellow color is the characteristic of silver NPs. The color of samples from water to NaCl solutions with different concentration gradually became darker and more opaque. As will be discussed, the color of NPs suspensions depends on their size and concentration of NPs in the solutions.

In metal NPs such as in silver, the conduction band and valence band lie very close to each other in which electrons move freely. These free electrons give rise to a surface plasmon

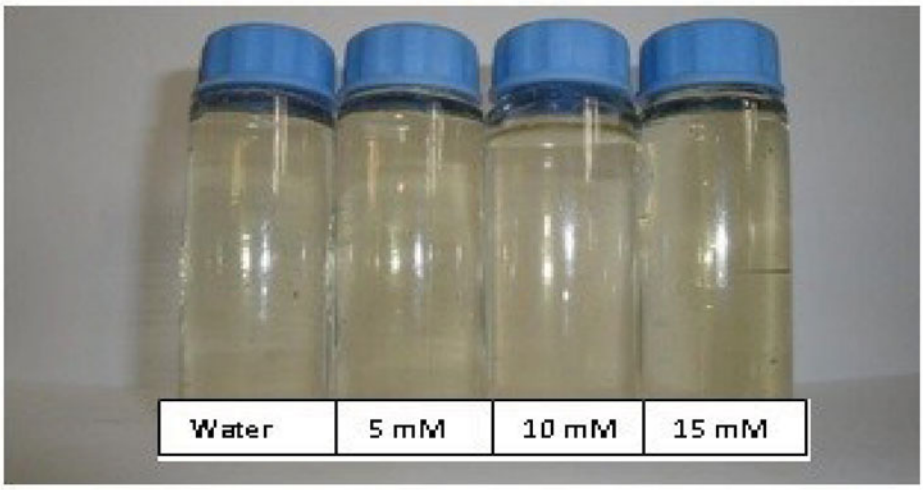

Figure 2. Ag NPs samples in distilled water and NaCl solution with different concentration.

resonance (SPR) absorption band [19–21], occurring due to the collective oscillation of electrons of silver NPs in resonance with the light wave [22]. Classically, the electric field of an incoming wave induced a polarization of the electrons with respect to much heavier ionic core of silver NPs. As a result, a net charge difference occurs which in turn acts as a restoring force. This creates a dipolar oscillation of all the electrons with the same phase [23].

When the frequency of the electromagnetic field tends to resonant with the coherent electron motion, a strong absorption take place, which is the origin of the observed color. Here the color of the prepared silver NPs is light yellow. The color of samples from water to NaCl solutions with different concentration gradually became darker and more opaque but the darkening of the solutions is not clear. The color of solution depends up on the size of NPs. The reason that the color of solutions do not change is that the sizes of NPs are in the same range and do not differ in samples.

The ablated mass is shown in Fig. 3. With increasing the concentration of NaCl in the solution, the ablated mass is decreased linearly. So because of the absorption and the pressure of the ablated environment, if the impurities of the ablated environment increase, the ablated rate will decrease.

The spectrum of absorption in the range of 200 to 1100 nm is shown in Fig. 4. The silver NPs have the main peak around 400 nm and this peak is associated with SPR. Shifts in the position of SPR peak may represent particle size variation. According to Mie and Drud theory, the shift towards shorter wavelength (blue shift) of the prepared nanoparticle indicates a decreased particle size and vise versa. Plasmonic peaks indicate that the silver NPs produced in NaCl solution with different concentration is smaller than the NPs produced in distilled water. With increasing the concentration on NaCl, the particle size is increased. The peaks at 970 nm correspond to silver oxide. The wavelengths corresponds to plasmonic peaks from water to 5 mM, 10 mM, and 15 mM of NaCl solution is 410 nm, 402 nm, and 404 nm, respectively. Blue shift of peak position from NPs spectrum in water to 5 mM is due to smaller size of NPs produced in NaCl solution. With increasing the

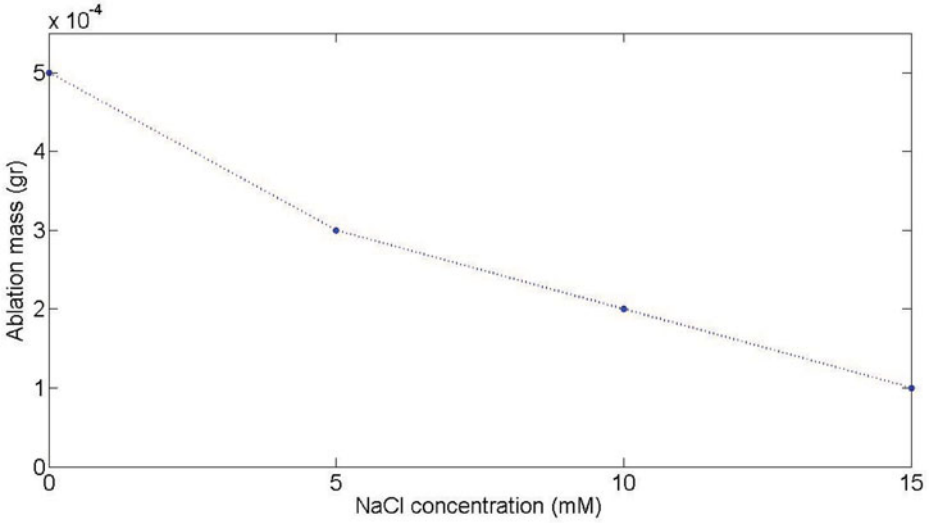

Figure 3. Variation of the ablated mass of the target during the ablation versus different concentrations NaCl solutions.

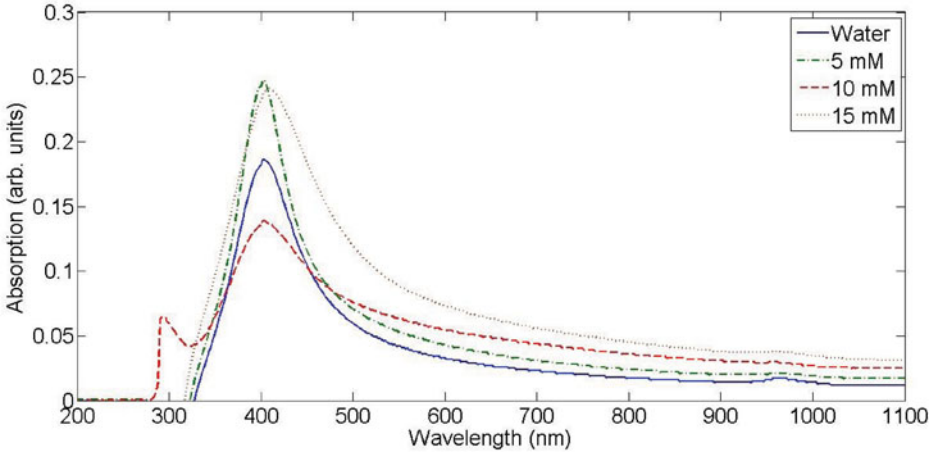

Figure 4. UV–Vis-NIR absorption spectrum of Ag NPs in distilled water and NaCl solutions with different concentration.

NaCl concentration, the size of NPs is increased. So we have the small shift toward larger wavelength in the plasmonic peaks.

The XRD pattern of target and dried powder of generated NPs is shown in Fig. 5. XRD spectrum presents the formation of the silver crystalline structure in NPs. Diffraction peaks are clearly observed and are located in positions consistent with those expected for Ag and AgCl, as indicated by the Joint Committee on Powder Diffraction Standards (JCPDS) plot presented beneath the experimental data. The preferred orientation of Ag bulk target and generated NP samples are almost different. All have a polycrystal structure with several preferred orientations. Therefore, it can be claimed that in this regime of ablation Ag atoms bond break by laser pulse energy so we can observe new recombination between atoms during the cooling process of plasma generated on the surface of the target. In addition, the mean grain size of synthesized Ag NPs could be estimated according to the Debye–Scherrer equation. Broadening the peaks of XRD pattern of NPs in comparison

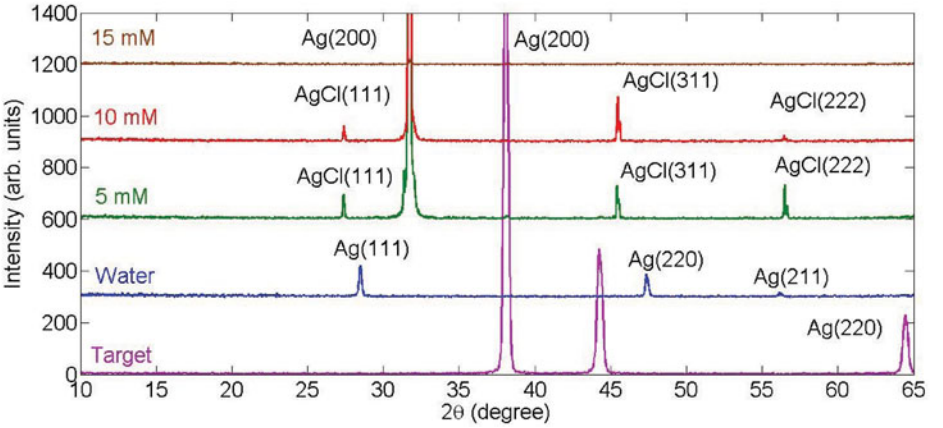

Figure 5. X-ray diffraction pattern of Ag NPs samples after drying.

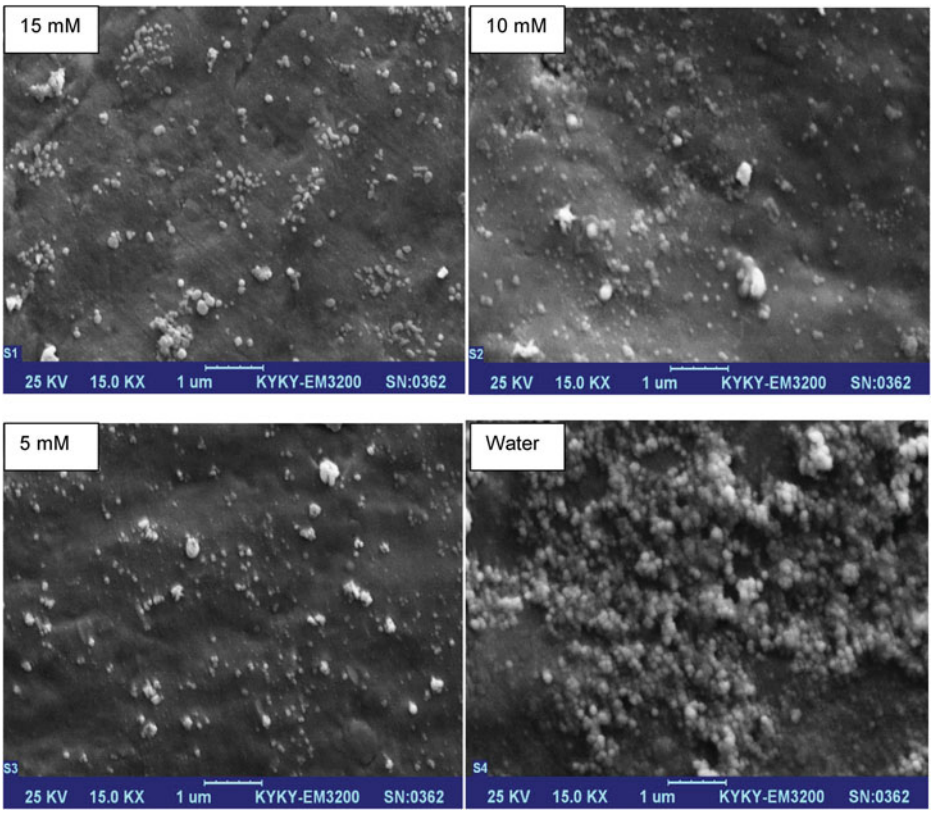

Figure 6. SEM image of Ag NPs in distilled water and NaCl solution with different concentrations.

with bulk peaks confirm that size of grains is decreased in the generated NPs in comparison with bulk Ag [24].

The XRD peaks in the wide angle range of 2θ ($10 < 2\theta < 65$) ascertains in the structure of nanoparticles in NaCl solution with concentration of 5, 10, and 15 mM (200), and (311) surfaces are formed while in the structure of nanoparticles in NaCl solution with concentration of 5 and 10 mM (222), (111), and (220) surface are generated. In NaCl solution with concentration of 5 and 10 mM, all the peaks are related to compounds of AgCl but in NaCl solution with concentration of 15 mM in addition to AgCl compounds, there is a peak (200) crystalline structure that is related to Ag NPs. So the formation of NPs in the NaCl solution in this experimental condition has been done with nucleation process. Nucleation process is a process in which the silver atoms are removed from target and in the laser ablation process they combine with Cl atoms in the plasma plume on the target surface. It is important to indicate that in 5 mM and 10 mM NaCl solutions, the intensity of XRD patterns peaks are in order of 1000 but in the distilled water and 15 mM NaCl solutions are in order of 100, it means that the intensity of 5 mM and 10 mM NaCl solution have extremely high degree of crystalline.

Figure 6 presents 15 k $\times$ magnification SEM images of Ag nanostructures prepared by laser ablation in distilled water and NaCl solutions with different concentration of NaCl. Images are prepared with 25 keV electrons. NPs solutions were dried on Al foil at room temperature before imaging. The generated grains of NPs in this experimental condition

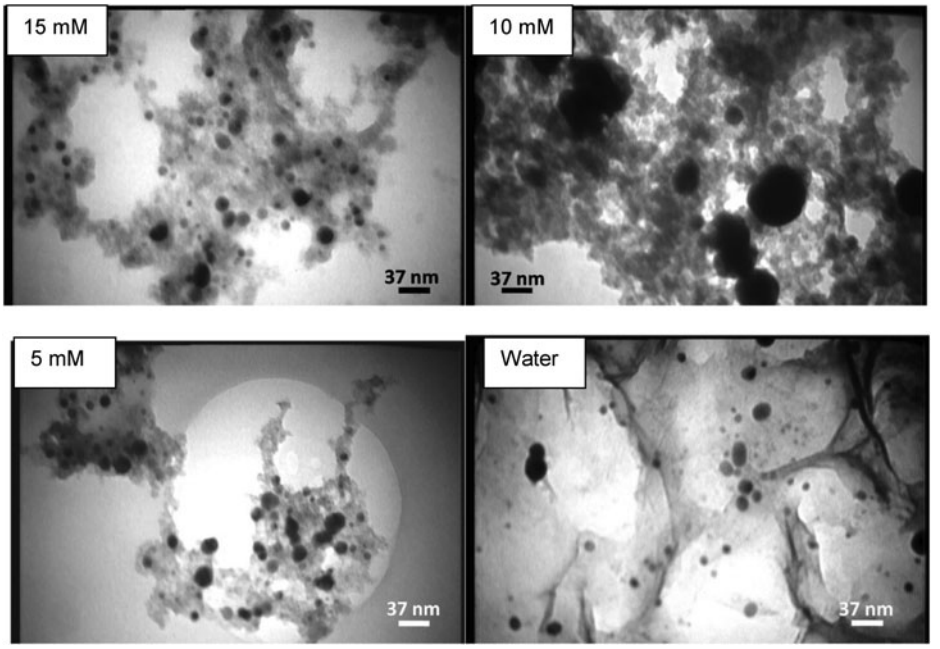

Figure 7. TEM image of Ag NPs generated in distilled water and NaCl solution with different concentration with laser ablation mechanism.

are spherical and adhered to each other. NPs are adhered to each other and grains are formed. It is observable that with the number of NPs that adhered to each other in distilled water is more than NaCl solutions. There isn't any difference in the number of Ag NPs that are produced in NaCl solutions with different concentration. It is obvious that the size of NPs in NaCl solutions is smaller than distilled water, whereas with increasing the NaCl concentration the size of NPs is increased.

The size distribution of the silver NPs has been measured by TEM micrographs. For TEM imaging, a drop of the solution is deposited and dried on a carbon-coated copper grid. Figure 7 shows the TEM photograph of Ag NPs and Fig. 8 shows the particle size distribution of silver NPs, obtained from TEM analysis. For the particle size distribution, we calibrate the software according to the specified magnification. Then with regard to the population of particles, we draw the column charts. As can be seen, the silver NPs are spherical in all samples.

They are so small that cannot be seen clearly even with high resolution TEM. The largest particles are formed in the water and the size of NPs which are produced in NaCl solution is smaller than the particles which are produced in water that seems to have the highest concentration.

DynamicLightScattering (DLS) measures the hydrodynamic radius of NPs in solution and provides information on the aggregation state of NPs in solution. In fact the hydrodynamic diameter of NPs is the total size of the particle size plus electrostatic potential radius around them. In fact by DLS measurement, we obtain the radius of a sphere that NPs locate at its center and at the edge of the sphere electrostatic potential tends to zero. In the polar solutions, the difference between real radius and electrostatic potential is larger. For DLS measurement, samples were irradiated with electromagnetic wave of 633 nm wavelength.

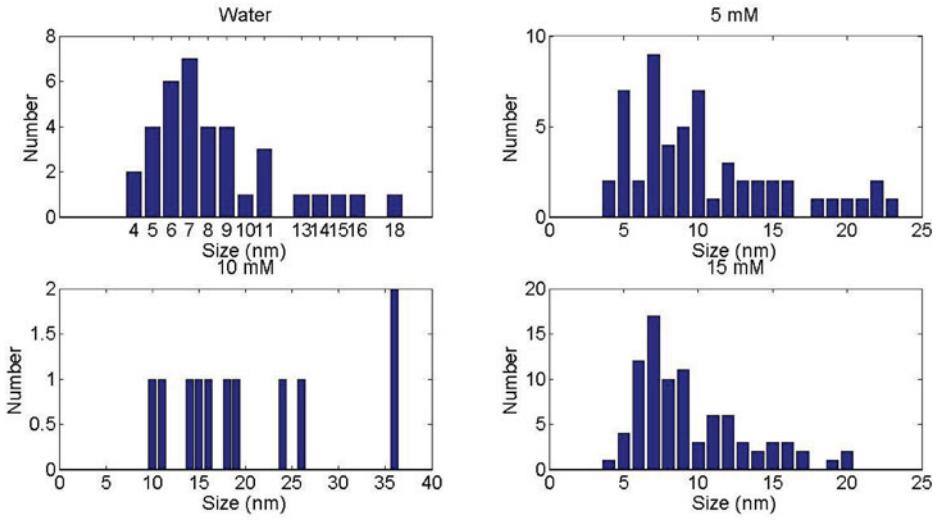

Figure 8. Particle size distribution of Ag NPs generated in distilled water and NaCl solutions with laser ablation mechanism.

In Fig. 9, the size distribution of samples measured by DLS is shown. The maximum number of NPs in water is 13 nm in diameter and in 5 mM NaCl solution they are 16 nm and 20 nm. In 10 mM NaCl solution, most of NPs are 18 nm and in 15 mM NaCl solution they are 20 nm. With increasing the NaCl concentration, the size of NPs became larger. There isn't any noticeable difference between hydrodynamic radius of NPs in distilled water and 5 mM NaCl solution, but difference of hydrodynamic radius of NPs from 5 mM NaCl solution to 15 mM NaCl solution is noticeable. It is because of the polarization of ablation environment. Because of low accuracy of the DLS from other analysis, we cannot observe the NPs under 10 nm.

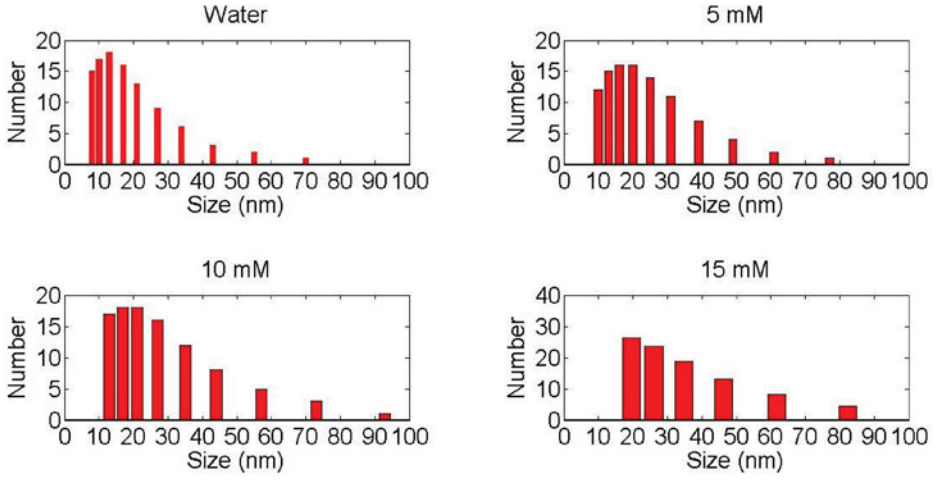

Figure 9. Ag NPs hydrodynamic size distribution of samples measured by Dynamic Light Scattering (DLS) device.

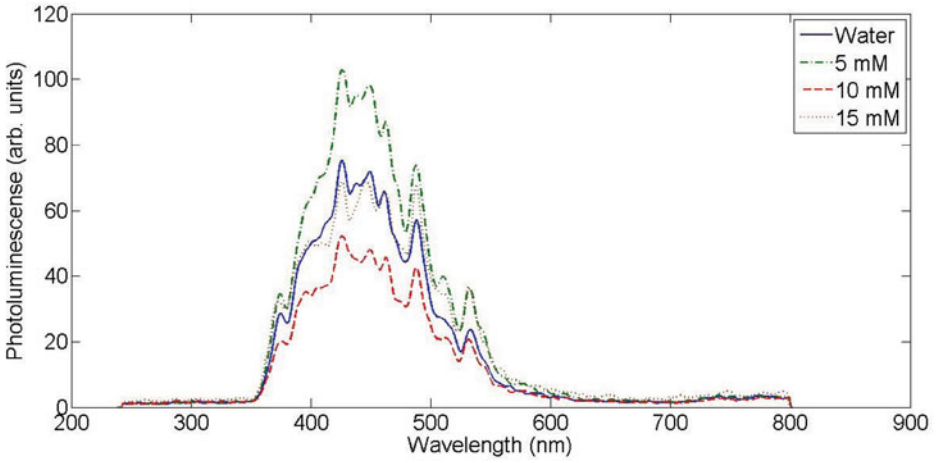

Figure 10. Photoluminescence spectra of Ag NPs in NaCl solutions.

The PL from noble metal NPs was reported for silver NPs [25,26]. These measurements revealed the maximum of the PL band close to the interband absorption edge and thus the PL was attributed to the interband radiative transitions [25,26]. The PL was observed only from NPs smaller than 20 nm in diameter and from nanorods with a high aspect ratio, which suggests a strong size and morphology dependence of the PL spectra. When the size of the particles decreased, the intensity of the PL increased indicating a strong influence of the surface the NPs have on the PL spectra.

The photoluminescence spectra from Ag NPs are shown in Fig. 10. Photoluminescence emissions spectra from the synthesized samples have been recorded at room temperature at 220 nm excitation wavelength. The photoluminescence peaks of samples are between 426 nm to 427 nm. The range between 300 nm to 550 nm refers to electron–hole recombination. The schematic of the excitation and recombination mechanisms can be depicted as shown in Fig. 11, where the band structure for a typical noble metal is represented by a simple model. Excitation occurs from states in upper *d*-bands to level and above the Fermi energy. Because of the small photon momentum, the interband transition is assumed to be

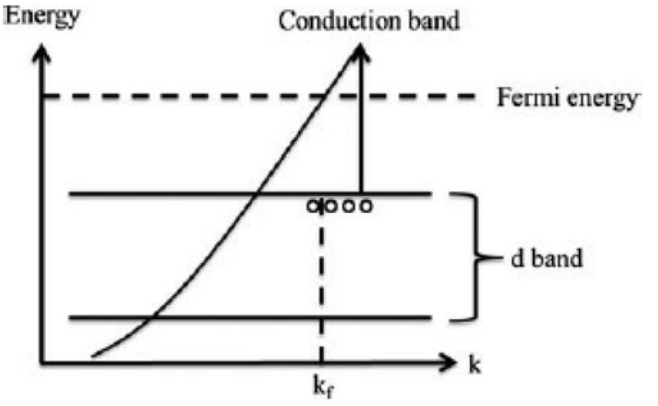

Figure 11. Excitation and recombination mechanism inside the band structure of noble metals.

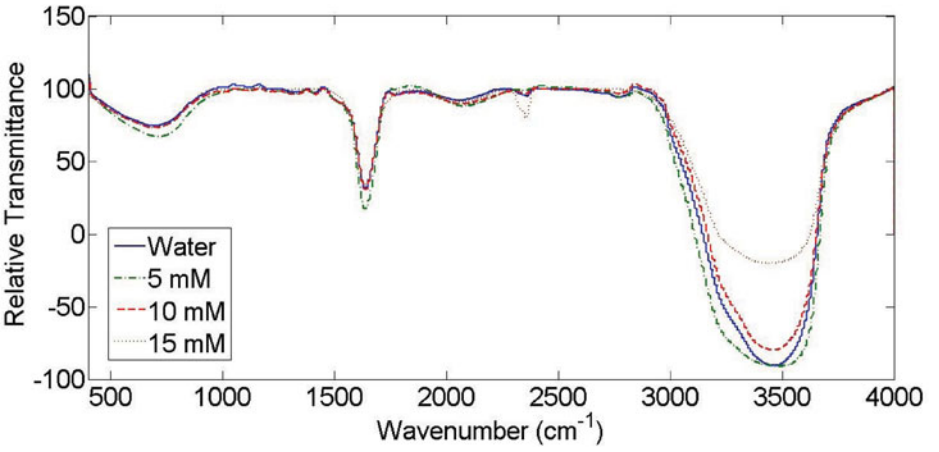

Figure 12. FTIR of Ag NPs in distilled water and NaCl solutions with different concentration.

direct. The emission arises from direct recombination of conduction band electron below the Fermi energy with holes in the *d*-band that have scattered to momentum state less than the Fermi momentum K_F [27]. When the excitation energy is high enough, the electrons in the *d*-bands have a probability to be excited if the vacant states in the conduction band exists and holes are created in *d*-bands. However, if the recombination process occurs later, these holes first move closer to the conduction band electrons near the Fermi surface. Subsequent electron–phonon and hole–phonon scattering process leads to an energy loss and finally recombination of an electron from an occupied *sp* band with a hole in the *d*-band takes place [28].

Even if the excitation is carried out in the plasmon band, rapid relaxation to the interband transition must take place. Electrons and holes relax by phonon scattering processes and some recombine radiatively to give rise to the observed luminescence. Such an intrinsic emission profile is, however, modified by the local field induced around the NPs owing to excitation of the plasmon resonance [29].

The FTIR spectra of samples are shown in Fig. 12. These spectra are measured between 400 cm^{-1} to 4000 cm^{-1}. The peak ranging from 3200–3600 cm^{-1} is attributed to presence of O—H stretching vibration [30] that with increasing the concentration of NaCl, the intensity of peaks is decreased. The broad peak ranging from 1500–1700 cm^{-1} can be explained owing by the O—H flexural vibration of water [30] that the intensity of this peak is larger than others. The peak ranging from 2300–2400 cm^{-1} is attributed to presence of C═O band [30] because the samples are dried in outdoors and except 5 mM NaCl solutions the others have the same intensity. The peak ranging from 600–800 cm^{-1} is attributed to the presence of silver oxide band.

4. Conclusion

In this work, the effect of NaCl concentration on the production of silver NPs prepared by PLA of Ag metal plate in distilled water and NaCl solutions with different concentrations is investigated. The generated NPs in this experimental condition are spherical. Concentration of Ag NPs in distilled water is higher than the concentration of Ag NPs particles in NaCl solutions.

With adding NaCl to ablation environment, the morphology of produced NPs do not change and their aggregation decreases so the size of NPs in NaCl solutions is smaller than the size of NPs in distilled water, and so there is a good agreement between TEM and SEM and DLS analysis. XRD data reveal that AgCl will be produced in the solutions with very high degree of crystallinity. Although the preferred orientation of Ag target and produced NPs are different but the preferred orientation of lattice in NPs is independent of the amount of NaCl in the ablation environment.

References

[1] Mafune, F., Kohno, J., Takeda, Y., Kondow, T., & Sawabe, H. (2001). *J. Physics. Chem. B*, *105*, 5114.
[2] He, S., Yao, J., Jiang, P., Shi, D., Zhang, H., Xie, S., Pang, S., & Gao, H. (2001). *Langmuir*, *17*, 1571.
[3] Yang, G. W. (2007). *Prog. Mater. Sci. 52*, 648–698.
[4] Imam, H., Elsayed, K. H. A., Ismail, L. Z., Afify, M., & Atta Khedr, M. (2013). *J. Life. Sci.*, *10*(4) 401.
[5] Diao, J. J., Sun, J. W., & Hutchison, J. B. (2005). *Appl. Phys. Lett.*, *87*, 103.
[6] Song, C. X., Wang, D. B., Lin, Y. S., Hu, Z. S., Gu, G. H., & Fu, X. (2004). *Nanotechnology*, *15*, 962.
[7] Heath, J. R. (1989). *Phys. Rev. B*, *40*, 9982.
[8] Kawabata, A., & Kubo, R. (1966). *J. Phys. Soc. Jpn.*, *21*, 1765.
[9] Eustis, S., Krylova, G., Eremenva, A., Schill, A. W., & EL-Sayed, M. (2005). *Photochem. Photobiol. Sci.*, *4*, 154.
[10] Bohren, C. F., & Huffman, D. R. (1998). *Absorption and Scattering of Light by Small Particles*, Wiley: NewYork.
[11] Creighton, J. A., & Eadon, D. G. (1991). *J. Chem. Soc. Faraday Trans.*, *87*, 3881.
[12] Pastoriza-Santos, I. & Liz-Marzan, L. M. (2002). *Nano Lett.*, *2*, 903.
[13] Tsuji, M., Hashimoto, M., Nishizawa, Y., Kubokawa, M., & Tsuji, T. (2005). *Chem. Eur. J.*, *11*, 440.
[14] Wiley, B., Sun, Y., Mayers, B., & Xia, Y. (2005). *Chem. Eur. J.*, *11*, 454.
[15] Takami, A., Kurata, H., & Koda, S. (1999). *J. Phys. Chem. B*, *103*, 1226.
[16] Link, S., Mohamed, M. B., Nikoobakht, B., & El-Sayed, M. A. (1999). *J. Phys. Chem.*, *103*, 1165.
[17] Link, S., Wang, Z. L., & El-Sayed, M. A. (2000). *J. Phys. Chem. B*, *104*, 7867.
[18] Link, S., & El-Sayed, M. A. (2001). *J. Chem. Phys.*, *114*, 2362.
[19] Taleb, A., Petit, C., & Pileni, M. P. (1998). *J. Phys. Chem. B*, *102*, 2214.
[20] Noginov, M. A., Zhu, G., Bahoura, M., Adegoke, J., Small, C., Ritzo, B. A., Drachev, V. P., & Shalaev, V. M. (2008). *Appl. Phys. Lett. 92*, 043101.
[21] Link, S., & El-Sayed, M. A. (2003). *Annu. Rev. Phys. Chem.*, *54*, 331.
[22] Nath, S. S., Chakdar, D., & Gope, G. (2007). *Nanotrends*, *2*, 321.
[23] Yousef, J., Hendi, H., Hakami, F. S., Awad, M. A., Alem, A. F., Hendi, A. A., Ortashi, K., & Al- Mrshoud, M. F. (2012). *J. Am. Sci.*, *8*(3), 589.
[24] Pyatenko, A., Shimokawa, K., Yamaguchi, M., Nishimura, O., & Suzuki, M. (2004). *Appl. Phy. A: Mat. Sci. Proc.*, *79*, 803.
[25] Zhang, P., Zhang, J. Z., & Fang, Y. (2008). *J. Lumin. 128*, 1635.
[26] Basak, D., Karan, S., & Mallik, B. (2006). *Chem. Phys. Lett.*, *420*, 115.
[27] Fayaz, M., Tiwary, C. S., Kalaichelvan, P. T., & Venkatesan, R. (2010). *Colloids Surf. B, Biointerfaces*, *75*, 175–178.
[28] Desarkar, H. S., Kumbhakar, P., & Mitra, A. K. (2013). *J. Lumin.*, *134*, 1. ‘
[29] Link, S., & El-Sayed, M. A. (2000). *Int. Rev. Phys. Chem.*, *19*(3), 409.
[30] Solati, E., Dorranian, D., & Dejam, L. (2012). *Appl. Phys A.*, *109*, 307.